PCCP

PAPER

View Article Online
View Journal | View Issue

Cite this: *Phys. Chem. Chem. Phys.*, 2023, **25**, 975

Magnetic field effects on radical pair reactions: estimation of $B_{1/2}$ for flavin-tryptophan radical pairs in cryptochromes†

Siu Ying Wong, ‡[a] Philip Benjamin‡[b] and P. J. Hore *[b]

Received 17th August 2022,
Accepted 4th December 2022

DOI: 10.1039/d2cp03793a

rsc.li/pccp

Magnetic field effects on the yields of radical pair reactions are often characterised by the "half-field" parameter, $B_{1/2}$, which encodes useful information on spin relaxation, radical recombination kinetics and electron-electron couplings as well as electron–nuclear hyperfine interactions. Here we use a variety of spin dynamics simulation methods to estimate the hyperfine-only values of $B_{1/2}$ for the flavin-tryptophan radical pair, [$FAD^{\bullet-}$ $TrpH^{\bullet+}$], thought to be the detector in the magnetic compass sense of migratory songbirds. The main findings are: (a) in the absence of fast recombination and spin relaxation, [$FAD^{\bullet-}$ $TrpH^{\bullet+}$] radical pairs in solution and in the putative magnetoreceptor protein, cryptochrome, have $B_{1/2} \approx 1.89$ mT and 2.46 mT, respectively. (b) The widely used expression for $B_{1/2}$ due to Weller *et al.* (*Chem. Phys. Lett*, 1983, **96**, 24–27) is only applicable to small, short-lived (~5 ns), rapidly tumbling radical pairs in solution, and is quantitatively unreliable in the context of magnetoreception. (c) In the absence of molecular tumbling, the low-field effect for [$FAD^{\bullet-}$ $TrpH^{\bullet+}$] is predicted to be abolished by the anisotropic components of the hyperfine interactions. Armed with the 2.46 mT "base value" for cryptochrome, measurements of $B_{1/2}$ can be used to understand the impact of spin relaxation on its performance as a magnetic compass sensor.

Introduction

Radical pairs are short-lived reaction intermediates with the unusual property that their chemistry can be influenced by magnetic interactions orders of magnitude smaller than the thermal energy, k_BT (Boltzmann's constant times temperature).[1–4] A combination of spin-selective reactivity, relatively slow spin relaxation, and electron–nuclear hyperfine interactions leads to the coherent interconversion of the electronic singlet and triplet states of the pair which can be affected by applied magnetic fields as weak as ~50 μT.[5,6] As a result, the yields of the reaction products, $\Phi(B)$, are frequently found to depend sigmoidally on the strength of the applied magnetic field, B.[7–10] This behaviour is often characterised by a parameter, $B_{1/2}$, defined as the magnetic field at which $\Phi(B)$ is mid-way between the reaction yield at zero field and the "saturation" value at high field (Fig. 1a):

$$\Phi(B_{1/2}) = \tfrac{1}{2}[\Phi(0) + \Phi(\text{high field})]. \quad (1)$$

In some cases this "half-field" parameter is dominated by the hyperfine interactions in the radicals but there can also be contributions from fast recombination reactions,[9,10] spin relaxation processes,[12–14] paramagnetic–diamagnetic exchange,[15,16] and electron exchange and dipolar interactions.[17,18] It is therefore important to be able to estimate the hyperfine contribution to $B_{1/2}$ so that information on these other factors, about which less is usually known, can be extracted from experimental data. An equation due to Weller *et al.* has been widely used for this purpose.[7] For a pair of radicals, A and B:

$$B_{1/2}^{W} = 2\sqrt{3}\left(\frac{\sigma_A^2 + \sigma_B^2}{\sigma_A + \sigma_B}\right), \quad (2)$$

with effective hyperfine interactions σ_K in the two radicals given by:

$$\sigma_K = \sqrt{\frac{1}{3}\sum_k a_{k,K}^2 I_{k,K}(I_{k,K}+1)}. \quad (3)$$

In eqn (3), $a_{k,K}$ and $I_{k,K}$ are, respectively, the isotropic hyperfine coupling constant and the spin quantum number of nucleus k in radical K. The sum runs over all hyperfine-coupled nuclei in the radical. Weller *et al.* used eqn (2) to account for values of $B_{1/2}$ measured for a series of radical pairs formed in methanol and acetonitrile solutions by the photo-induced transfer of an electron from a variety of aromatic electron donors to the

[a] *Institut für Physik, Carl-von-Ossietzky Universität Oldenburg, Oldenburg 26111, Germany. E-mail: peter.hore@chem.ox.ac.uk*
[b] *Department of Chemistry, University of Oxford, Oxford, OX1 3QZ, UK*

† Electronic supplementary information (ESI) available. See DOI: https://doi.org/10.1039/d2cp03793a

‡ These authors contributed equally.

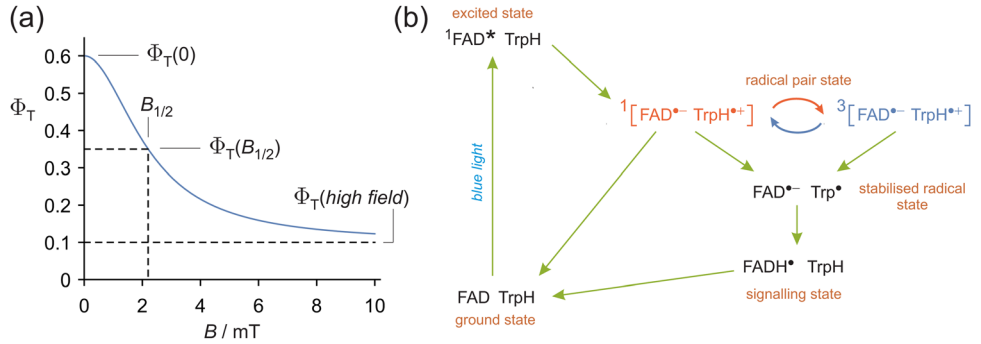

Fig. 1 (a) Schematic magnetic field effect on the fractional yield, $\Phi_T(B)$, of the product formed from the triplet state of a singlet-born radical pair. The applied magnetic field is assumed to be weak enough that effects arising from the Δg mechanism[1] are negligible. (b) Simplified photocycle of avian Cry4a.[11] The red and blue curly arrows represent the coherent singlet–triplet interconversion of the magnetically sensitive [FAD$^{\bullet-}$ TrpH$^{\bullet+}$] radical pair. FADH$^{\bullet}$ is the protonated form of FAD$^{\bullet-}$. Trp$^{\bullet}$ is the deprotonated form of TrpH$^{\bullet+}$. ^{1}FAD* is the excited singlet state of FAD.

tetracyclic aromatic hydrocarbon, pyrene.[7] The form of the expression was rationalised by asserting, without justification, that $B_{1/2}$ should be the weighted average of the two root-mean-square hyperfine couplings, $\sqrt{3}\sigma_A$ and $\sqrt{3}\sigma_B$, with weights equal to $\sigma_A/\bar{\sigma}$ and $\sigma_B/\bar{\sigma}$, respectively, where $\bar{\sigma} = \frac{1}{2}(\sigma_A + \sigma_B)$. Note that the definitions of σ_K and $B_{1/2}$ in ref. 7 did not use the factors of $\sqrt{3}$ in eqn (2) and (3).

Not only does eqn (2) have little basis in theory, it is also not the only empirical expression consistent with the $B_{1/2}$ measurements reported by Weller *et al.*[7] For example, the simpler expression,

$$B_{1/2} = 3.1\sqrt{\sigma_A^2 + \sigma_B^2}, \quad (4)$$

fits the data just as well as eqn (2) (ESI,† Section S1).

We are aware of only one attempt to test the accuracy of eqn (2). Rodgers *et al.*[19] used a quantum mechanical Monte-Carlo approach (QMMC) to calculate $\Phi(B)$ and hence $B_{1/2}$ for more than 12 000 radical pairs containing three spin-1/2 nuclei in each radical. The hyperfine couplings were chosen randomly such that σ_K for each radical was uniformly distributed between 0 and 0.75 mT. The study concluded that eqn (2) is best regarded as a useful, but not very accurate, rule of thumb for radical pairs with lifetimes in the range 10 to 100 ns. The discrepancies between eqn (2) and the QMMC results were more pronounced for both shorter and longer lived pairs.

Our purpose here is to assess in greater detail the accuracy of eqn (2) with a particular focus on the radical pair, [FAD$^{\bullet-}$ TrpH$^{\bullet+}$], thought to be the sensor in the light-dependent magnetic compass of migratory songbirds.[4,11,20–24] The radicals are formed within Cry4a, one of the six known avian cryptochrome proteins,[11,25–32] *via* photo-excitation of the flavin adenine dinucleotide (FAD) cofactor followed by sequential electron transfers along a chain of four tryptophan (TrpH) residues. Competition between singlet radical pair recombination and TrpH$^{\bullet+}$ deprotonation results in magnetic field effects on the quantum yield of a relatively long-lived form of the protein which could act as a signalling state (Fig. 1b).[11] The FAD$^{\bullet-}$ and TrpH$^{\bullet+}$ radicals in Cry4a are separated by ~2 nm and have dipolar and exchange interactions: $|D| \approx 300$–500 μT and $|J| \leq 2$ μT, respectively.[11]

In the following, we use spin dynamics simulations to estimate the contribution of isotropic hyperfine interactions to $B_{1/2}$ for the [FAD$^{\bullet-}$ TrpH$^{\bullet+}$] radical pair in cryptochrome for different radical pair lifetimes. We also treat the case of static, randomly oriented cryptochrome molecules for which anisotropic hyperfine and dipolar interactions cannot be ignored. A variety of approximate simulation methods have been deployed because of the computational challenges posed by an exact quantum mechanical treatment of a system of ~30 coupled spins comprising ~10^{10} spin states. The main aims are: (a) to assess the reliability of eqn (2) as a predictor of $B_{1/2}$, and (b) to determine the true contribution of hyperfine interactions to $B_{1/2}$ for [FAD$^{\bullet-}$ TrpH$^{\bullet+}$] as a basis for future studies of the effects of spin relaxation on its performance as a magnetic compass sensor.

Results

Weller equation

To evaluate eqn (2) for [FAD$^{\bullet-}$ TrpH$^{\bullet+}$] we used a complete set of isotropic hyperfine coupling constants, previously calculated using density functional theory.[33] A total of 27 nuclei were included (ESI,† Section S2): four ^{14}N and eleven ^{1}H in FAD$^{\bullet-}$ and two ^{14}N and ten ^{1}H in TrpH$^{\bullet+}$. Using eqn (3), the effective hyperfine interactions in the two radicals are σ_{FAD} = 0.70 mT and σ_{Trp} = 0.97 mT and hence $B_{1/2}^{W}$ = 2.97 mT. Note that this estimate includes no contribution from spin relaxation, fast recombination reactions, electron–electron couplings or anisotropic hyperfine interactions.

Schulten–Wolynes method

Schulten and Wolynes (SW) have proposed an approximate treatment of the spin dynamics of radical pairs in which the electron spins were considered to precess around the vector sum of the applied magnetic field and a time-independent magnetic field arising from the hyperfine interactions.[34] In the implementation used here (ESI,† Section S3), the latter was modelled by Monte-Carlo averaging over isotropic Gaussian distributions of hyperfine fields for each radical (mean zero, standard deviation σ_K).[35] Singlet and triplet pairs were

considered to react with the same first-order rate constant, k, to give distinct products (the "exponential model"[36]). The magnetic field effect was quantified by calculating the quantum yield, $\Phi_T(B)$, of the product formed from the triplet state of a singlet-born radical pair. $B_{1/2}$ was obtained by interpolating $\Phi_T(B)$ (ESI,† Sections S4 and S5). Exchange and dipolar interactions between the radicals and spin relaxation were not included. Applied to a radical pair comprising pyrene and *N*,*N*-dimethylaniline radicals, the SW approach was originally shown to give excellent agreement with exact quantum simulations.[34] It has subsequently been found to be less reliable at predicting the spin dynamics of long-lived radical pairs.[37,38]

Fig. 2 shows how $B_{1/2}$ calculated using the SW method varies with (a) $\sigma_{AB} = (\sigma_A^2 + \sigma_B^2)^{1/2}$, (b) σ_A/σ_B, and (c) k. Under the conditions of these calculations, detailed in the figure caption, a number of deviations from $B_{1/2}^W$ are immediately apparent. Both estimates of $B_{1/2}$ are proportional to σ_{AB} (Fig. 2a), but with different gradients: 2.11 for SW and $\sqrt{6} = 2.45$ for Weller. $B_{1/2}$ obtained using the SW method is approximately independent of the ratio σ_A/σ_B (Fig. 2b) while $B_{1/2}^W$ decreases markedly as σ_A/σ_B is increased towards 1.0. Versions of Fig. 2a and b, calculated for different values of k can be found in the ESI† (Section S5) together with representative plots of the field-dependence of $\Phi_T(B)$.

Finally, SW predicts that $B_{1/2}$ is approximately independent of k up to $\sim 5 \times 10^7$ s^{-1}, and then increases sharply for faster recombination rates (Fig. 2c). $B_{1/2}^W$, by contrast, is independent of k. Under the conditions of Fig. 2c, the two approaches agree when $k \approx 1.6 \times 10^8$ s^{-1}, *i.e.* when the radical pairs have a lifetime of ~ 6 ns.

For the cryptochrome-based radical pair, [FAD$^{\bullet-}$ TrpH$^{\bullet+}$], using the values of σ_{FAD} and σ_{Trp} quoted above, and $k = 10^6$ s^{-1}, we find $B_{1/2} = 2.51$ mT, approximately 15% smaller than $B_{1/2}^W$. Further discussion of this and other estimates of $B_{1/2}$ (collected together in Table 1) is deferred to the Discussion section.

Quantum mechanical Monte-Carlo method

We have extended the previous QMMC test of Weller's equation[19] by including up to seven spin-1/2 nuclei per radical. $\Phi_T(B)$ was calculated exactly, as described in ref. 19, and interpolated to obtain $B_{1/2}$ (ESI,† Sections S4 and S6). The hyperfine coupling constants for each radical were randomly chosen to be uniformly distributed between −1 mT and +1 mT and then scaled to obtain $\sigma_{FAD} = 0.70$ mT and $\sigma_{Trp} = 0.97$ mT. In all other respects, the calculations were performed under the same conditions as the SW simulations (isotropic hyperfine couplings, no exchange or dipolar interactions, equal singlet and triplet reaction rate constants, no spin relaxation).

Distributions of $B_{1/2}$ values for 1500 radical pairs containing 3, 4, 5, 6, or 7 nuclear spins per radical and $k = 10^6$ s^{-1} are shown in Fig. 3. As the number of nuclear spins was increased, both the mean and standard deviation decreased, with the mean tending towards ~ 2.0 mT, *i.e.* 33% smaller than $B_{1/2}^W$. The $B_{1/2}$ distributions for $k = 10^7$ s^{-1}, 10^8 s^{-1}, and 10^9 s^{-1} displayed similar behaviour with extrapolated means of 2.1, 2.5, and 6.6 mT, respectively (ESI,† Section S6).

Quantum dynamics method

The QMMC approach described above used random hyperfine coupling constants to achieve the appropriate values of σ_{FAD} and σ_{Trp}. A more direct approach would be to simulate the quantum dynamics (QD) in exactly the same way but using the actual hyperfine coupling constants of FAD$^{\bullet-}$ and TrpH$^{\bullet+}$. The challenge is that the dimensions of the matrices involved in the calculation scale exponentially with the number of spins in each radical, such that the calculations become impracticable for radical pairs with more than about $n_{nuc} = 15$ nuclei. We therefore performed a series of calculations in which the nuclear spins in FAD$^{\bullet-}$ and TrpH$^{\bullet+}$ were introduced one by one in approximate order of decreasing hyperfine coupling (ESI,† Section S2) in the hope that $B_{1/2}$ would cease to depend on n_{nuc} before the calculations became inconveniently slow or impossible (ESI,† Section S7).

The results are shown in Fig. 4a for several values of the recombination rate constant k and up to 15 nuclear spins. Although $B_{1/2}$ for the two smallest rate constants (10^6 and 10^7 s^{-1}) appears to

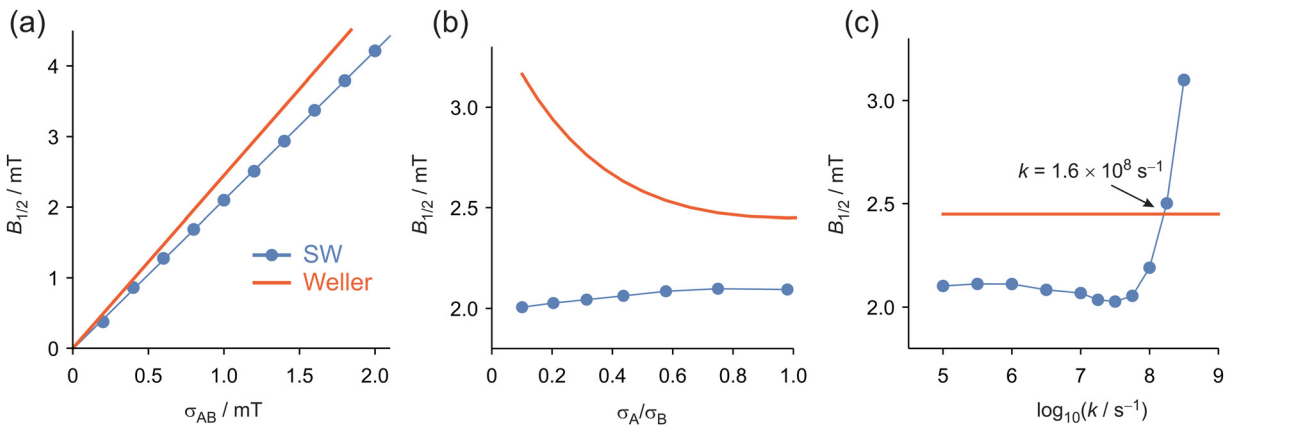

Fig. 2 $B_{1/2}$ calculated using the Schulten–Wolynes (SW) semiclassical method (blue) compared to $B_{1/2}^W$ obtained from eqn (2) (red). 50 000 Monte-Carlo samples of the hyperfine field distributions were used for the former. (a) $B_{1/2}$ as a function of σ_{AB} for $\sigma_A = \sigma_B$ and $k = 10^6$ s^{-1}. The blue line is the best linear fit to the calculated values of $B_{1/2}$ (gradient 2.11, intercept ≈ -0.11 mT). (b) $B_{1/2}$ as a function of σ_A/σ_B for $\sigma_{AB} = 1$ mT and $k = 10^6$ s^{-1}. (c) $B_{1/2}$ as a function of $\log_{10}k$ for $\sigma_{AB} = 1$ mT and $\sigma_A = \sigma_B$.

Table 1 Estimates of $B_{1/2}$ (in mT) for [FAD$^{\bullet-}$ TrpH$^{\bullet+}$]

Method	Weller[b]	SW[b]	QMMC[bc]	QD[d]	SC[e]
Isotropic HFI[a] $D = 0$	2.97	2.51	2.04	1.98	1.89

Method	Weller[f]	$SU(Z)$[g]
Anisotropic HFI[a] $D \neq 0$	3.71	2.46

[a] HFI: hyperfine interaction; D: dipolar interaction. $k = 10^6$ s^{-1}. [b] $\sigma_{FAD} = 0.70$ mT and $\sigma_{Trp} = 0.97$ mT. [c] Extrapolated from 3–7 nuclei per radical. [d] $n_{nuc} = 15$. [e] $n_{nuc} = 27$. [f] $\sigma_{FAD} = 1.03$ mT, $\sigma_{Trp} = 1.11$ mT. [g] Average over $n_{nuc} = 13$–16.

level out by the time $n_{nuc} = 15$, the same cannot be said for the four larger values of k. It appears that the shorter the lifetime of the radical pair, the more sensitive $B_{1/2}$ is to small hyperfine interactions.

The value of $B_{1/2}$ for $k = 10^6$ s^{-1} and $n_{nuc} = 15$ ($\sim$1.98 mT) is similar to the QMMC result (above) and 33% smaller than predicted by the Weller equation.

Improved semiclassical dynamics method

To include a larger number of nuclear spins than is feasible in the QD approach, we used an improved version of the SW method, denoted SC.[37] Rather than assuming that the sum of the nuclear spin vectors, weighted by the hyperfine couplings, is fixed in space, the SC method allows each nuclear spin in a radical to precess around the electron spin. In both cases, the electron spin simultaneously precesses around the total nuclear spin vector. Valid for radical pairs with no exchange or dipolar interactions, and equal singlet and triplet reaction rate constants, the computational effort increases only linearly with the number of nuclear spins, rather than exponentially as in an exact quantum mechanical calculation and approaches quantitative agreement with quantum mechanics as the number of nuclear spins increases.[37] Further details of the method are given in the ESI† (Section S3).

The SC results for $6 \leq n_{nuc} \leq 27$ are compared with the QD calculations in Fig. 4a. The improved semiclassical values of $B_{1/2}$ become independent of the number of nuclei for $n_{nuc} \geq 20$ but are larger than the exact values (by, at most, 0.12 mT for $n_{nuc} = 15$). This discrepancy reflects the approximate nature of the SC approach, the reliability of which should improve as n_{nuc} is increased. In agreement with this, we find that the QD values, when extrapolated exponentially to $n_{nuc} = \infty$, are a good match to the SC results for $n_{nuc} = 27$ (ESI,† Section S8).

As we found using the SW approach (Fig. 2c), $B_{1/2}$ is almost independent of k when $k \leq 10^7$ s^{-1} and then increases when the recombination is faster. Fig. 4b shows the SC values of $B_{1/2}$ for $n_{nuc} = 27$ as a function of k, together with the best linear fit: $B_{1/2}/\text{mT} \approx 2.02 + k/(2.15 \times 10^8\ \text{s}^{-1})$. The origin of this behaviour appears to be analogous to the lifetime-broadening seen in magnetic resonance spectra.[39] Under conditions of "slow exchange", the additional linewidth in an electron paramagnetic resonance spectrum arising from a chemical reaction with rate constant k is k/π (in Hz) or $k/2\gamma_e$ (in mT) where $\gamma_e = 1.76 \times 10^8$ mT^{-1} s^{-1} is the electron magnetogyric ratio. Consistent with this, the reciprocal of the gradient in Fig. 4b (2.15×10^8 mT^{-1} s^{-1}) is not far off $2\gamma_e$ (3.52×10^8 mT^{-1} s^{-1}).

Anisotropic interactions

All of the calculations reported above have been performed with isotropic hyperfine interactions and no radical–radical interactions. This is a good approximation when the radicals tumble rapidly in solution, such that the effects of anisotropic interactions average out, and when the radicals are far enough apart that, on average, their exchange and dipolar interactions are small. However, the FAD$^{\bullet-}$ and TrpH$^{\bullet+}$ radicals of interest here are embedded in cryptochrome, a large slowly tumbling protein, and are separated by a distance ($\sim$2 nm) at which the electron dipolar interaction cannot be neglected.[40] Hyperfine anisotropy and dipolar coupling must therefore be considered.

The effect of including the complete hyperfine tensors instead of their isotropic components can be estimated using a modified form of eqn (3) (ref. 41):

$$\sigma_K = \sqrt{\frac{1}{3}\sum_k \langle \alpha_{k,K}{}^2 \rangle I_{k,K}\left(I_{k,K}+1\right)} \qquad (5)$$

in which $\langle \alpha_{k,K}{}^2 \rangle$ is the mean squared eigenvalue of the hyperfine tensor of nucleus k in radical K. Eqn (5) is appropriate for randomly oriented radical pairs with no rotational motion and no dipolar coupling. Using hyperfine tensors previously calculated using density functional theory[33] (ESI,† Section S2), we find: $\sigma_{FAD} = 1.03$ mT, $\sigma_{Trp} = 1.11$ mT and, from eqn (2), $B_{1/2}^{W} = 3.71$ mT. These values are significantly larger than their isotropic counterparts: $\sigma_{FAD} = 0.70$ mT, $\sigma_{Trp} = 0.97$ and $B_{1/2}^{W} = 2.97$ mT.

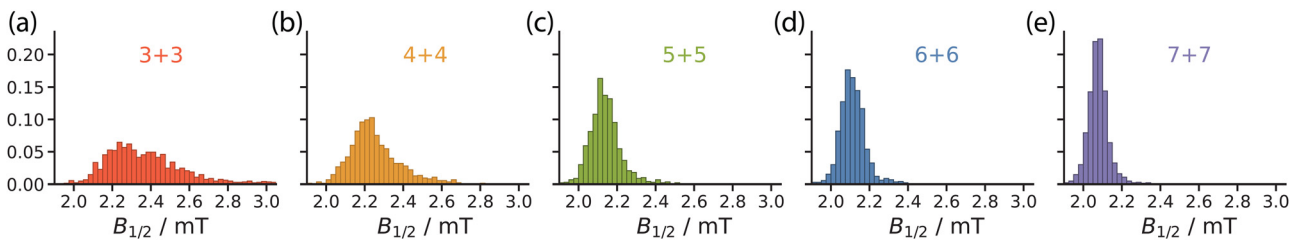

Fig. 3 $B_{1/2}$ distributions calculated using the QMMC method for model [FAD$^{\bullet-}$ TrpH$^{\bullet+}$] radical pairs containing 3, 4, 5, 6, or 7 hyperfine interactions per radical, as indicated.

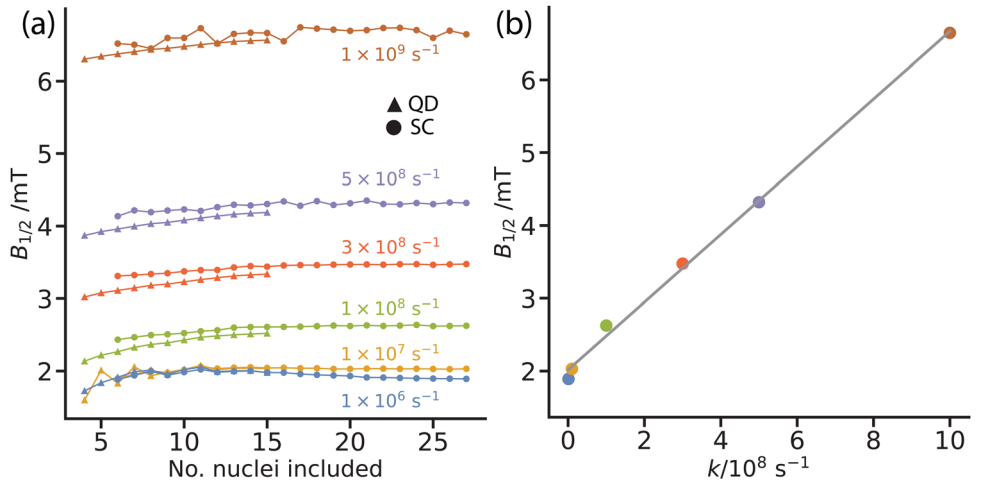

Fig. 4 (a) $B_{1/2}$ calculated for models of the [FAD$^{\bullet-}$ TrpH$^{\bullet+}$] radical pair. Nuclei were added one at a time in approximate order of decreasing hyperfine coupling. The recombination rate constants, k, are as indicated. Data are shown for exact quantum dynamics (QD, triangles, $4 \leq n_{\mathrm{nuc}} \leq 15$) and the improved semiclassical method (SC, circles, $6 \leq n_{\mathrm{nuc}} \leq 27$). (b) Best linear fit of the $B_{1/2}$ values for $n_{\mathrm{nuc}} = 27$ (SC method) as a function of k.

The simulation methods used above are either valid only when there are no exchange or dipolar interactions or take advantage of the absence of electron coupling to avoid using matrices with the dimension of the full spin space. To determine $B_{1/2}$ with anisotropic hyperfine and dipolar interactions included, we have used a method proposed by Fay *et al.* to model spin relaxation in radical pairs.[42] The initial singlet state of the radical pair was propagated in 1 ns time-steps to 5 μs and then integrated (using $k = 10^6$ s^{-1}) to obtain $\Phi_{\mathrm{T}}(B)$. The initial nuclear spin space was trace-sampled using a single $SU(Z)$ coherent state[42] with averaging over 16 randomly distributed directions of the magnetic field. The relative orientation of the two radicals and the dipolar coupling parameter ($D = -0.511$ mT) were appropriate for FAD and Trp318 in the crystal structure of pigeon cryptochrome 4a.[32] We refer to this method here as $SU(Z)$ (instead of stochastic Schrödinger equation, SSE[42]) because we do not use it to model spin relaxation.

Fig. 5 shows values of $B_{1/2}$ calculated using the $SU(Z)$ method for $n_{\mathrm{nuc}} = 7$–16, introducing the nuclei one at a time in the same order as before (ESI,† Sections S2 and S9). As in Fig. 4a, $B_{1/2}$ for isotropic hyperfine interactions and no dipolar interaction is a little less than 2.0 mT for $n_{\mathrm{nuc}} = 14$–16. When the anisotropic hyperfine components and the dipolar interaction were included, $B_{1/2}$ increased to ∼2.46 mT. This is substantially smaller than the estimate using eqn (2) and (5), $B_{1/2}^{\mathrm{W}} = 3.71$ mT.

The individual effects of the two anisotropic interactions are also shown in Fig. 5. Inclusion of just the dipolar coupling causes a small reduction in $B_{1/2}$ which is more than outweighed by the increase arising from the hyperfine anisotropy.

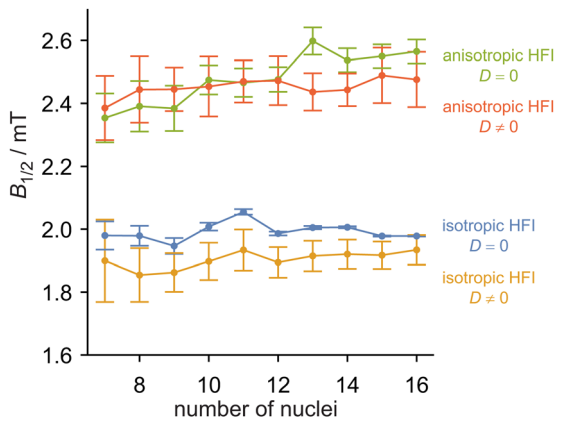

Fig. 5 $B_{1/2}$ calculated using the $SU(Z)$ method for models of the [FAD$^{\bullet-}$ TrpH$^{\bullet+}$] radical pair with $k = 10^6$ s^{-1}. The solid lines and error bars represent the mean ± standard deviation of the values for 16 randomly chosen magnetic field directions. In the purely isotropic case, the standard deviations arise from the use of a single, randomly chosen, $SU(Z)$ state in the stochastic trace sampling procedure and scale as $Z^{-1/2}$ where Z is the dimensionality of the nuclear spin Hilbert space. For the other three cases, the standard deviations are dominated by the anisotropic effects of the hyperfine and/or dipolar interactions.

Discussion

We have explored the validity of eqn (2) as a predictor of $B_{1/2}$, using a range of simulation methods, concentrating on the [FAD$^{\bullet-}$ TrpH$^{\bullet+}$] radical pair in cryptochrome because of its potential role as the magnetic compass sensor in migratory songbirds.[4] Table 1 collects together our estimates of $B_{1/2}$ for this radical pair when it recombines with a rate constant of 10^6 s^{-1}. A 1 μs lifetime is probably about optimal for magnetoreception: any shorter and there would be insufficient time for the Earth's magnetic field (∼50 μT) to influence the spin dynamics and any longer would risk attenuating the magnetic sensitivity through spin relaxation.[4,43–45] However, since $B_{1/2}$ is hardly affected by the recombination kinetics when $k < 10^7$ s^{-1} (Fig. 4), the precise value of k is not important for our assessment of the reliability of the Weller equation in the context of magnetoreception.

Weller equation

Compared to quantum and semiclassical spin dynamics simulations, the Weller equation is seen to be unreliable, both

qualitatively (Fig. 2b and c) and quantitatively (Table 1). To some extent, this is expected. Eqn (2) was originally proposed to rationalise the effects of magnetic fields on the chemistry of small, freely diffusing, rapidly tumbling radicals in non-viscous solutions. It is therefore not surprising that eqn (2) cannot account for the effects of anisotropic hyperfine interactions or radical–radical interactions. However, even with these limitations, eqn (2) is still found wanting. As judged by the calculations presented here, it consistently overestimates $B_{1/2}$. (Table 1) under conditions of slow ($k < 10^7$ s^{-1}) recombination.

The only circumstances under which eqn (2) agrees with our simulations is for a narrow range of much shorter lifetimes. For a radical pair with σ_{AB} = 1 mT, the SW approach (Fig. 2c) agrees with eqn (2) when $k \approx 1.6 \times 10^8$ s^{-1} while the SC method (Fig. 4b) only gives Weller's value of $B_{1/2}$ for [FAD$^{\bullet-}$ TrpH$^{\bullet+}$] when $k \approx 2.0 \times 10^8$ s^{-1}. This suggests that eqn (2) may only be applicable to radical pairs comprising small radicals in solution with lifetimes of the order of 5 ns.

This conclusion seems to be supported by a study of one of the radical pairs for which Weller's equation was originally proposed. Rodgers *et al.* measured magnetic field effects on the photochemical reactions of *N*,*N*-dimethylaniline with pyrene in which neither, one or both of the reactants had been perdeuterated.[19] By exploiting the different hyperfine interactions of the four isotopologues, it was possible to estimate the radical encounter times that were most effective for the generation of magnetic field effects. Encounters within 2 ns of radical pair formation contributed little because there was insufficient time for the applied magnetic field to affect the spin dynamics. Encounters at times longer than 10 ns were also ineffectual because of their low probability. The conclusion of Rodgers *et al.*[19] that only encounters on a 2–10 ns timescale are important for the magnetic sensitivity of the pyrene + *N*,*N*-dimethylaniline reaction agrees well with the finding here that eqn (2) works best when $k^{-1} \approx 5$ ns.

Comparison of simulation methods

We have simulated magnetic field effects on [FAD$^{\bullet-}$ TrpH$^{\bullet+}$] for two extreme cases: (A) fast rotational tumbling (such that anisotropic interactions are averaged to zero) with extensive translational diffusion (such that radical–radical interactions can be neglected), and (B) static, randomly oriented radical pairs with non-zero anisotropic (hyperfine and dipolar) interactions.

Table 1 presents the estimated values of $B_{1/2}$, in order of increasing sophistication of the method used to simulate the magnetic field effects. The SW semiclassical approach is known to be of limited reliability for the long-lived ($\sim$1 μs) radical pairs of interest here.[37,38] QMMC and QD treat the quantum spin dynamics exactly but are restricted in the number of nuclear spins that can be included and so require extrapolation to estimate $B_{1/2}$ for the intact 29-spin system of [FAD$^{\bullet-}$ TrpH$^{\bullet+}$]. Introducing the dipolar coupling would restrict the number of nuclear spins even further. The computational effort required for the improved semiclassical method, SC, increases linearly with the number of nuclear spins, allowing all 27 isotropic hyperfine interactions to be modelled reasonably accurately. However, this approach is only applicable when there is no electron-electron coupling. Finally, the *SU*(*Z*) method, for which the computational effort scales as $D \log D$ (with $D = 4Z$ being the size of the full electron–nuclear Hilbert space), is compatible with a reasonably large number of nuclei with dipolar coupling included.

Cryptochrome $B_{1/2}$

The best estimates of $B_{1/2}$ for [FAD$^{\bullet-}$ TrpH$^{\bullet+}$] are (Table 1): 1.89 mT for case (A) (isotropic hyperfine interactions, no dipolar coupling, SC method) and 2.46 mT for case (B) (anisotropic hyperfine interactions, non-zero dipolar coupling, no rotational motion, *SU*(*Z*) method). The majority of the difference between the two arises from the anisotropic components of the hyperfine interactions which outweigh a small reduction in $B_{1/2}$ caused by the dipolar interaction of FAD$^{\bullet-}$ and TrpH$^{\bullet+}$.

Case (B) above is more appropriate than case (A) for cryptochrome, a molecule with molecular mass $\sim$64 kDa. Under the conditions of the experiments used to measure $B_{1/2}$ for this protein (typically 20 : 80 glycerol : water mixtures at 5 °C[11]), the rotational correlation time τ_c of an avian Cry4a is estimated to be $\sim$80 ns (ESI,† Section S10). With this value, $\gamma_e \Delta B \tau_c = 1$ when ΔB = 0.1 mT implying that only anisotropic interactions (ΔB) smaller than $\sim$0.1 mT would be efficiently averaged by such slow tumbling. Both the anisotropic hyperfine interactions and the dipolar coupling in [FAD$^{\bullet-}$ TrpH$^{\bullet+}$] are considerably larger than 0.1 mT and would therefore not be much affected by rotational motion of the protein in solution.

The ''baseline'' value of $B_{1/2}$ for [FAD$^{\bullet-}$ TrpH$^{\bullet+}$] in Cry4a, resulting from anisotropic hyperfine and dipolar interactions alone, should therefore be taken as 2.46 mT.

Low-field effects

Finally, we consider the related issue of why ''low-field effects'' are not more commonly observed for cryptochrome-based radical pairs. The low-field effect is a characteristic of radical pairs that have long-lived spin coherence and manifests as a biphasic field-dependence of the reaction yield.[36] Typically, for a singlet-born radical pair, $\Phi_T(B)$ rises as B is increased from zero and then falls once B is comparable to or larger than σ_{AB}. The existence of a low-field effect has been interpreted as an indication that a radical pair could be suitable for detection of magnetic fields as weak as the Earth's ($\sim$50 μT), for which spin-coherence times of at least $\sim$1 μs are required.[12,46]

Fig. 6a shows $\Phi_T(B)$ in the range $0 \leq B \leq 2$ mT for [FAD$^{\bullet-}$ TrpH$^{\bullet+}$], calculated using the *SU*(*Z*) approach for case (A) (isotropic hyperfine interactions and no dipolar interaction) with n_{nuc} = 14, $k = 10^6$ s^{-1}. A weak but distinct low-field effect is clearly visible below $\sim$0.5 mT. The fairly steep gradient of $\Phi_T(B)$ at B = 0, implies a reasonably large sensitivity to Earth-strength magnetic fields. However, the corresponding calculation for case (B) (anisotropic hyperfine and non-zero dipolar interactions, no rotational motion) in Fig. 6d has no suggestion of a low-field effect. Fig. 6b (isotropic hyperfine and non-zero dipolar interactions) and Fig. 6c (anisotropic hyperfine and

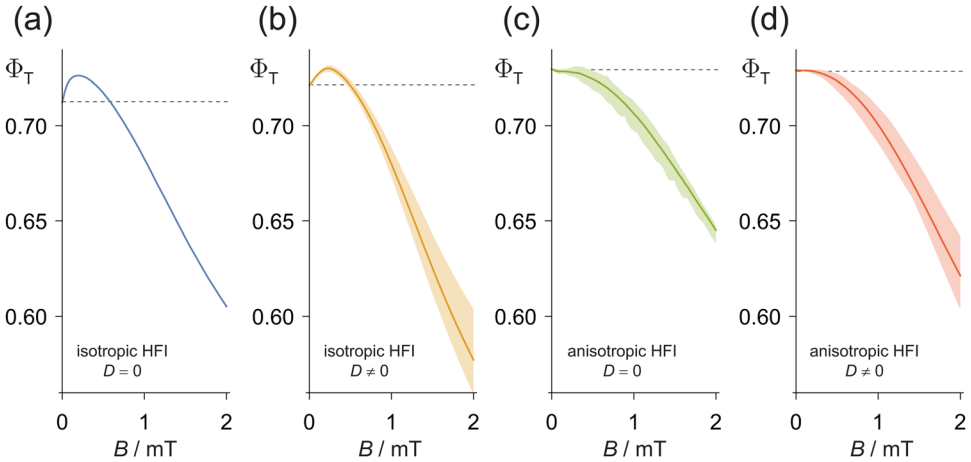

Fig. 6 $\Phi_T(B)$ calculated for [FAD$^{\bullet-}$ TrpH$^{\bullet+}$] using the *SU*(*Z*) approach. (c and d) include anisotropic components of the hyperfine interactions. (b and d) include a dipolar interaction ($D = -0.511$ mT). The low-field effect is clearly visible in (a and b) as a small rise in $\Phi_T(B)$ at fields below ~0.5 mT. The solid lines represent $\Phi_T(B)$ averaged over 16 random magnetic field directions. The shaded regions show the range of $\Phi_T(B)$ values for the different field directions.

no dipolar interactions) show that it is the hyperfine anisotropy rather than the dipolar coupling that abolishes the low-field effect in these simulations.

The correspondence between this prediction and experimental measurements of magnetic field effects on cryptochromes is unclear. Small low field effects have been reported for a plant cryptochrome (*Arabidopsis thaliana* cryptochrome 1, *At*Cry1) and the structurally related DNA photolyase from *E. coli* (*Ec*PL).[12] If other magnetically sensitive members of the cryptochrome-photolyase family have low field effects, they have so far been too small to detect. These proteins include both wild-type and W369F mutant versions of European robin (*Erithacus rubecula*) cryptochrome 4a (*Er*Cry4a)[11] and the cryptochrome from the fruit fly *Drosophila melanogaster* (*Dm*Cry).[47] The measurements for *At*Cry1 and *Ec*PL were made at 260 or 270 K in 50 : 50 or 60 : 40 glycerol : water mixtures. Those for *Er*Cry4a and *Dm*Cry were done at 278 K in 20 : 80 glycerol : water solutions. Given the lower viscosity of the *Er*Cry4a and *Dm*Cry samples, one might have expected a larger low field effect as a result of the more efficient averaging of anisotropic components of the hyperfine interactions. Nor can the absence of a low field effect in *Er*Cry4a and *Dm*Cry be attributed to the additional tryptophan in the electron transfer chains of these proteins because the W369F mutant of *Er*Cry4a, which lacks the terminal tryptophan residue of the Trp-tetrad, shows no discernible low field effect. Further experiments will be required to resolve the apparent discrepancy with the simulations in Fig. 6.

Conclusions

A number of conclusions emerge from this study. First, it appears that Weller's expression for $B_{1/2}$ is only applicable to small, short-lived (~5 ns), rapidly tumbling radical pairs in solution. It is unreliable for both longer and shorter lifetimes and/or in situations where anisotropic hyperfine and/or exchange/dipolar interactions affect the spin dynamics. Second, the hyperfine-only value of $B_{1/2}$ for the [FAD$^{\bullet-}$ TrpH$^{\bullet+}$] radical pair in cryptochrome in solution is ~2.46 mT. The observation of $B_{1/2}$ values larger than this should be taken as a strong indication that additional factors, such as electron spin relaxation, are at play. Third, for reactions of free flavin and tryptophan radicals in non-viscous solution, the corresponding value of $B_{1/2}$ is ~1.89 mT. Fourth, the low-field effect for [FAD$^{\bullet-}$ TrpH$^{\bullet+}$] pairs in cryptochromes in solution is predicted to be abolished by the anisotropic components of the hyperfine interactions. These insights will be valuable in future studies of the effects of spin relaxation on the performance of [FAD$^{\bullet-}$ TrpH$^{\bullet+}$] as a magnetic compass sensor.

Conflicts of interest

There are no conflicts to declare.

Acknowledgements

We are grateful to the following for financial support: the European Research Council (under the European Union's Horizon 2020 research and innovation programme, grant agreement no. 810002, Synergy Grant, QuantumBirds), the Office of Naval Research Global (award no. N62909-19-1-2045), and the Deutsche Forschungsgemeinschaft, project no. 395940726 (SFB 1372, Magnetoreception and Navigation in Vertebrates).

References

1 U. E. Steiner and T. Ulrich, *Chem. Rev.*, 1989, **89**, 51–147.
2 C. T. Rodgers, *Pure Appl. Chem.*, 2009, **81**, 19–43.
3 A. R. Jones, *Molec. Phys.*, 2016, **114**, 1691–1702.
4 P. J. Hore and H. Mouritsen, *Annu. Rev. Biophys.*, 2016, **45**, 299–344.

5 K. Maeda, K. B. Henbest, F. Cintolesi, I. Kuprov, C. T. Rodgers, P. A. Liddell, D. Gust, C. R. Timmel and P. J. Hore, *Nature*, 2008, **453**, 387–390.
6 C. Kerpal, S. Richert, J. G. Storey, S. Pillai, P. A. Liddell, D. Gust, S. R. Mackenzie, P. J. Hore and C. R. Timmel, *Nat. Commun.*, 2019, **10**, 3707.
7 A. Weller, F. Nolting and H. Staerk, *Chem. Phys. Lett.*, 1983, **96**, 24–27.
8 M. E. Michel-Beyerle, R. Haberkorn, W. Bube, E. Steffens, H. Schröder, H. J. Neusser, E. W. Schlag and H. Seidlitz, *Chem. Phys.*, 1976, **17**, 139–145.
9 M. E. Michel-Beyerle, H. W. Krüger, R. Haberkorn and H. Seidlitz, *Chem. Phys.*, 1979, **42**, 441–447.
10 H. J. Werner, K. Schulten and A. Weller, *Biochim. Biophys. Acta*, 1978, **502**, 255–268.
11 J. Xu, L. E. Jarocha, T. Zollitsch, M. Konowalczyk, K. B. Henbest, S. Richert, M. J. Golesworthy, J. Schmidt, V. Déjean, D. J. C. Sowood, M. Bassetto, J. Luo, J. R. Walton, J. Fleming, Y. Wei, T. L. Pitcher, G. Moise, M. Herrmann, H. Yin, H. Wu, R. Bartölke, S. J. Käsehagen, S. Horst, G. Dautaj, P. D. F. Murton, A. S. Gehrckens, Y. Chelliah, J. S. Takahashi, K.-W. Koch, S. Weber, I. A. Solov'yov, C. Xie, S. R. Mackenzie, C. R. Timmel, H. Mouritsen and P. J. Hore, *Nature*, 2021, **594**, 535–540.
12 K. Maeda, A. J. Robinson, K. B. Henbest, H. J. Hogben, T. Biskup, M. Ahmad, E. Schleicher, S. Weber, C. R. Timmel and P. J. Hore, *Proc. Natl. Acad. Sci. U. S. A.*, 2012, **109**, 4774–4779.
13 U. E. Steiner and J. Q. Wu, *Chem. Phys.*, 1992, **162**, 53–67.
14 E. A. Weiss, M. A. Ratner and M. R. Wasielewski, *J. Phys. Chem. A*, 2003, **107**, 3639–3647.
15 M. Justinek, G. Grampp, S. Landgraf, P. J. Hore and N. N. Lukzen, *J. Am. Chem. Soc.*, 2004, **126**, 5635–5646.
16 K. Schulten, *J. Chem. Phys.*, 1985, **82**, 1312–1316.
17 R. Haberkorn, M. E. Michel-Beyerle and R. A. Marcus, *Proc. Natl. Acad. Sci. U. S. A.*, 1979, **76**, 4185–4188.
18 A. Ogrodnik, H. W. Kruger, H. Orthuber, R. Haberkorn, M. E. Michelbeyerle and H. Scheer, *Biophys. J.*, 1982, **39**, 91–99.
19 C. T. Rodgers, S. A. Norman, K. B. Henbest, C. R. Timmel and P. J. Hore, *J. Amer. Chem. Soc.*, 2007, **129**, 6746–6755.
20 S. Y. Wong, Y. Wei, H. Mouritsen, I. A. Solov'yov and P. J. Hore, *J. R. Soc., Interface*, 2021, **18**, 20210601.
21 S. Y. Wong, A. Frederiksen, M. Hanic, F. Schuhmann, G. Grüning, P. J. Hore and I. A. Solov'yov, *Neuroforum*, 2021, **27**, 141–150.
22 N. Karki, S. Vergish and B. D. Zoltowski, *Protein Sci.*, 2021, **30**, 1521–1534.
23 R. Kavet and J. Brain, *Physiology*, 2021, **36**, 183–194.
24 T. Ritz, S. Adem and K. Schulten, *Biophys. J.*, 2000, **78**, 707–718.
25 T. Hochstoeger, T. Al Said, D. Maestre, F. Walter, A. Vilceanu, M. Pedron, T. D. Cushion, W. Snider, S. Nimpf, G. C. Nordmann, L. Landler, N. Edelman, L. Kruppa, G. Durnberger, K. Mechtler, S. Schuechner, E. Ogris, E. P. Malkemper, S. Weber, E. Schleicher and D. A. Keays, *Sci. Adv.*, 2020, **6**, eabb9110.
26 N. Ozturk, C. P. Selby, S. H. Song, R. Ye, C. Tan, Y. T. Kao, D. P. Zhong and A. Sancar, *Biochemistry*, 2009, **48**, 8585–8593.
27 A. Günther, A. Einwich, E. Sjulstok, R. Feederle, P. Bolte, K.-W. Koch, I. A. Solov'yov and H. Mouritsen, *Curr. Biol.*, 2018, **28**, 211–223.e214.
28 H. Wu, A. Scholten, A. Einwich, H. Mouritsen and K.-W. Koch, *Sci. Rep.*, 2020, **10**, 7364.
29 A. Einwich, K. Dedek, P. K. Seth, S. Laubinger and H. Mouritsen, *Sci. Rep.*, 2020, **10**, 15794.
30 H. Mitsui, T. Maeda, C. Yamaguchi, Y. Tsuji, R. Watari, Y. Kubo, K. Okano and T. Okano, *Biochemistry*, 2015, **54**, 1908–1917.
31 X. Wang, C. Jing, C. P. Selby, Y.-Y. Chiou, Y. Yang, W. J. Wu, A. Sancar and J. Wang, *Cell. Molec. Life Sci.*, 2018, **75**, 4629–4641.
32 B. D. Zoltowski, Y. Chelliah, A. Wickramaratne, L. Jarocha, N. Karki, W. Xu, H. Mouritsen, P. J. Hore, R. E. Hibbs, C. B. Green and J. S. Takahashi, *Proc. Natl. Acad. Sci. U. S. A.*, 2019, **116**, 19449–19457.
33 A. A. Lee, J. C. S. Lau, H. J. Hogben, T. Biskup, D. R. Kattnig and P. J. Hore, *J. R. Soc., Interface*, 2014, **11**, 20131063.
34 K. Schulten and P. G. Wolynes, *J. Chem. Phys.*, 1978, **68**, 3292–3297.
35 K. Maeda, T. Miura and T. Arai, *Mol. Phys.*, 2006, **104**, 1779–1788.
36 C. R. Timmel, U. Till, B. Brocklehurst, K. A. McLauchlan and P. J. Hore, *Mol. Phys.*, 1998, **95**, 71–89.
37 D. E. Manolopoulos and P. J. Hore, *J. Chem. Phys.*, 2013, **139**, 124106.
38 T. P. Fay, L. P. Lindoy, D. E. Manolopoulos and P. J. Hore, *Faraday Discuss.*, 2020, **221**, 77–91.
39 P. J. Hore, *Nuclear magnetic resonance*, Oxford University Press, Oxford, 2015.
40 N. S. Babcock and D. R. Kattnig, *J. Phys. Chem. Lett.*, 2020, **11**, 2414–2421.
41 V. I. Borovkov, V. A. Bagryansky, G. A. Letyagin, I. V. Beregovaya, L. N. Shchegoleva and Y. N. Molin, *Chem. Phys. Lett.*, 2018, **712**, 208–213.
42 T. P. Fay, L. P. Lindoy and D. E. Manolopoulos, *J. Chem. Phys.*, 2021, **154**, 084121.
43 D. R. Kattnig, I. A. Solov'yov and P. J. Hore, *Phys. Chem. Chem. Phys.*, 2016, **18**, 12443–12456.
44 S. Worster, D. R. Kattnig and P. J. Hore, *J. Chem. Phys.*, 2016, **145**, 035104.
45 D. R. Kattnig, J. K. Sowa, I. A. Solov'yov and P. J. Hore, *New J. Phys.*, 2016, **18**, 063007.
46 F. Cintolesi, T. Ritz, C. W. M. Kay, C. R. Timmel and P. J. Hore, *Chem. Phys.*, 2003, **294**, 385–399.
47 D. M. W. Sheppard, J. Li, K. B. Henbest, S. R. T. Neil, K. Maeda, J. Storey, E. Schleicher, T. Biskup, R. Rodriguez, S. Weber, P. J. Hore, C. R. Timmel and S. R. Mackenzie, *Sci. Rep.*, 2017, **7**, 42228.

